Microfluidics

DOI: 10.1002/anie.201403256

Versatile Preparation of Nonspherical Multiple Hydrogel Core PAM/PEG Emulsions and Hierarchical Hydrogel Microarchitectures**

*Song Guo, Tong Yao, Xiaobo Ji, Changfeng Zeng, Chongqing Wang, and Lixiong Zhang**

Abstract: *The preparation of nonspherical materials composed of separated multicomponents by droplet-based microfluidics remains a challenge. Based on polymerization-induced phase separation and droplet coalescence in microfluidics, we prepared emulsions of variously shaped PAM/PEG core/shell droplets and hydrogels composed of two separated components, which show flexible and transformable hierarchical structures and microarchitectures. We find that AM/PEG aqueous droplets form a core/shell structure after polymerization resulting from phase separation. Thus multicore/shell droplets are easily produced by coalescence of core/shell structures. By changing the polymerization temperature and the flow rate, the morphology of the multicore droplets and the hydrogel can be easily adjusted. The hydrogels exhibit apparent anisotropy and different protein release rates depending on their structures. The preparation technique is simple and versatile and the resulting hydrogels have potential applications in many fields.*

Microfluidic techniques have developed rapidly in the past two decades because of the flow features in microchannels and versatile manipulation of liquids.[1,2] Of these techniques, droplet-based microfluidics has received broad attention in many areas, as these droplets can be used as independent microreactors and are able to transport, mix, react, and be analyzed separately.[3] Various microfluidic devices ranging from simple T-junctions[4] to complex capillary-constructed assemblies[5–7] are applied to form droplets, enabling the fabrication of complex/multiple emulsions,[5–8] monodisperse particles,[9,10] Janus particles,[11–13] hollow spheres,[9,14,15] nonspherical colloidosomes,[16] etc. However, these preparations require the careful choice and adjustment of the surfactants,[17] precise design and assembly of microfluidic devices,[5–8,18] and modification of the microchannels' surface wettability[8,18] for the formation of droplets inside the microdevices. Furthermore, most of the materials prepared in droplet-based microfluidics are of spherical geometry.

Irregular-shaped materials with hierarchical microarchitectures are of great interest owing both the fundamental understanding of their formation from simple starting materials and their various potential applications, e.g. in self-assembly,[19] drug delivery,[20,21] cell encapsulation,[22,23] and tissue engineering.[24a] This stimulates the fabrication of anisotropically shaped manufactured microparticles. On the other hand, microparticles consisting of nonspherical particles or nonspherical and mixed-shaped particles have recently attracted much attention.[25] Although some bottom-up and top-down methods have been developed to produce these microparticles,[24b,c] a challenge remains in terms of reproducibility and simplicity. Microfluidics-based techniques may provide a simple and easy route to fabricate such spherical and nonspherical mixed-shaped particles. However, there have been limited reports on the preparation of hierarchical microarchitectures using droplet-based microfluidics.[16,25–33] Examples include nonspherical SiO_2 colloidosomes fabricated by evaporation of the oil in the middle layer of water-oil-water (W/O/W) emulsions;[16] nonspherical SiO_2/ethoxylated trimethylolpropane triacrylate composite microcapsules generated by encapsulating emulsion droplets in photocurable shell droplets based on an optofluidic platform;[28] ovular shaped poly(1,6-hexanediol dimethacrylate)/polyacrylamide hydrogels obtained by shrinkage of Janus particles;[29] and dumbbell-shaped hybrid Janus microspheres prepared by merging one organic droplet with an inorganic one, followed by a photo-initiated polymerization.[30] Apparently, these particles either show unique geometry but consist of a single component, or they are created from two components but show a simple configuration. Nonspherical microarchitectures with a complex geometry composed of two separated components are seldom prepared by microfluidic techniques, suggesting that their preparation by droplet-based microfluidics remains a challenge.

We describe the preparation of various single- to multicore/shell emulsions and hydrogels composed of two separated components, which show flexible and transformable hierarchical structures and microarchitectures, using the droplet-based microfluidic technique. We first fabricate hydrogel/water/oil (H/W/O) emulsions consisting of a polyacrylamide (PAM) hydrogel core surrounded by poly(ethylene glycol) (PEG) in paraffin in a simple co-flow microfluidic device. The fabrication is based on polymerization-induced phase separation of PAM from PEG during the polymeri-

[*] S. Guo, T. Yao, X. B. Ji, Prof. C. Q. Wang, Prof. L. X. Zhang
State Key Laboratory of Materials-Oriented Chemical Engineering
College of Chemistry and Chemical Engineering
Nanjing Tech University
Nanjing 210009 (P. R. China)
E-mail: lixiongzhang@yahoo.com
Prof. C. F. Zeng
College of Mechanical and Power Engineering
Nanjing Tech University
Nanjing 210009 (P. R. China)

[**] This work is supported by Natural Science Key Project of the Jiangsu Higher Education Institutions (12KJA530002), the Priority Academic Program Development of Jiangsu Higher Education Institutions, and the Research and Innovation Program for College Postgraduates of Jiangsu Province (No. CXLX12_0456). PAM = polyacrylamide, PEG = poly(ethylene glycol).

Supporting information for this article is available on the WWW under http://dx.doi.org/10.1002/anie.201403256.

zation of acrylamide (AM) in a homogeneous solution of AM and PEG.[34] We later fuse several single-core droplets to prepare emulsions with multicore droplets and then convert them to core-containing PAM/PEG hydrogels by merging the droplet with a polymerizable poly(ethylene glycol)diacrylate (PEGDA) droplet also in a simple microfluidic device. We can transform the spherical hydrogel particles to several kinds of nonspherical ones by conducting the polymerization of PEGDA at different temperatures and treating the particles under different conditions. The nonspherical PAM/PEG hydrogels show anisotropy in the adsorption of rhodamine B and CdTe quantum dots, thus exhibiting red and green color at different spots of the hydrogel. Besides, the different structures of these hydrogels influence the release rates of protein. This preparation technique is simple and versatile and the resultant multicore/shell droplet emulsions and hydrogels can be finely tuned in fine structure and morphology.

We conducted the experiments using a simple co-flow microdevice to generate an aqueous droplet by shearing an aqueous phase from an oil phase without addition of any surfactant (Experimental Section in the Supporting Information, SI). The aqueous phase comprises PEG, AM, *N*,*N*′-methylene bisacrylamide (MBAM, as a cross-linking agent), ammonium persulfate (APS, as an initiator), and H_2O; the compositions are listed in Table S1. The oil phase is liquid paraffin. The obtained aqueous droplet flows with the oil phase along a 0.3×500 mm polytetrafluoroethylene (PTFE) tube, which is immersed in a water bath so that AM can be polymerized at high temperatures. To obtain the spherical microdroplets, aqueous- and oil-phase flow rates of 0.3 and 1.5 mL h^{-1}, respectively, are applied with the residence time of 80 s. The resultant droplets prepared at 96, 93, 90, and 87 °C (entries S1–S4, Table S1, SI) show uniform spherical morphology and a core/shell structure, with a mean diameter of ca. 300 μm, as observed by optical microscope (Figure 1 a). The core is believed to be PAM, which is formed by the heat treatment and separates from PEG. To verify this, we separated the cores from the emulsions by charging them in ethanol and examined the obtained microspheres by IR spectroscopy. Their fine structures were investigated using scanning electron microscopy (SEM) (Figure S4, SI). The core is opaque, as the core is a PAM-rich phase with a porous network that exhibits low light transparency. This is the result of interference processes in combination with refractive index differences between the various components. The core diameter of the droplets decreases from 4/5 to 2/5 when the polymerization temperature is decreased from 96 to 87 °C. This can be explained by a lower conversion at lower polymerization temperatures (the conversions are 98, 85, 72, and 40 % at 96, 93, 90, and 87 °C, respectively), which results in limited phase separation.[34] Thus we can adjust the size of the core by choosing the appropriate polymerization temperature, consequently changing the morphologies of the multicore/shell droplet emulsions and hydrogels, as will be shown later. Furthermore, the amount of MBAM has a certain influence on the formation of the H/W/O emulsions and their morphologies. Additionally, the PEG content can influence the size of the core (Figure S3, SI).

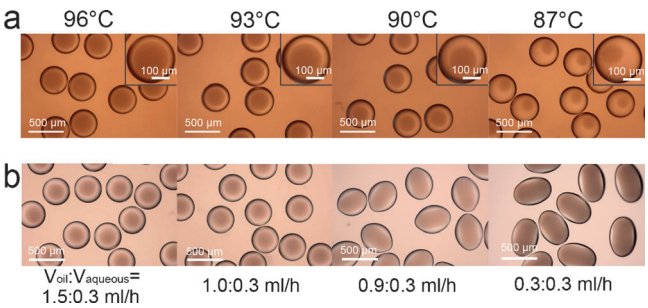

Figure 1. Optical microscopy images of the single-core H/W/O droplet emulsions prepared a) at different temperatures and b) with different oil-phase/aqueous-phase flow rate ratios. The MBAM and PEG concentrations are 4 wt % and 10 wt %, respectively. Scale bars: 500 μm. Scale bars in insets: 100 μm.

As the flow pattern of the droplet can be easily tuned by changing the velocity of the continuous phase,[35a] we investigated the effect of oil-phase flow rate on the morphology of both the core and the emulsion. When the oil-phase flow rate was decreased from 1.5 to 1.0 mL h^{-1} (the aqueous-phase flow rate was kept at 0.3 mL h^{-1}), the resulting H/W/O emulsion droplets still exhibit spherical morphology; however, some cores in the emulsions changed from a spherical to a bullet-like shape. As the flow rate was further decreased to 0.9 and 0.3 mL h^{-1}, we obtained oval-shaped H/W/O emulsion droplets containing rod-shaped cores, with a slight increase in the aspect ratio of the rod from 1.9 to 2.1 (Figure 1 b).

Since no surfactant is used in the system, coalescence of droplets can be easily accomplished. Thus, we can prepare multicore H/W/O emulsions by fusing the above single-core droplets in an expanding straight channel[35b] connected to the outlet of the PTFE tube by increasing the aqueous-phase flow rate (Experimental Section 3.2, SI). We first merged two to four single spherical core droplets under the conditions listed in Table S1 at the polymerization temperature of 87 °C (entries S11–S13, SI). We found that with increasing aqueous-phase flow rate, two to four single-core H/W/O emulsion droplets can be merged to form spherical multiple H/W/O droplets containing two to four hydrogel cores (Movies S1–S4, SI; Figure 2 a). When we conducted the preparation at polymerization temperatures of 90 and 93 °C, multiple H/W/O emulsion droplets containing two to four hydrogel cores also formed, showing vesica piscis, Reuleaux triangle, and quadrangle shapes for the double-, triple-, and quadruple-core-containing emulsion droplets, respectively (Figure 2 a). This can be explained by formation of small-sized cores at a polymerization temperature of 87 °C and large-sized cores at 90 and 93 °C.

We also merged two to four rodlike core droplets prepared above to form multicore H/W/O emulsion droplets. They show morphologies quite different from those of their spherical-core counterparts, exhibiting square-like, pentagon-like, and hexagon-like droplets for double, triple, and quadruple rodlike core-containing H/W/O droplets, respectively (Figure 2 b). Thus we can change the morphology of the H/W/O emulsion droplets easily by choosing different polymerization temperatures and oil-phase flow rates.

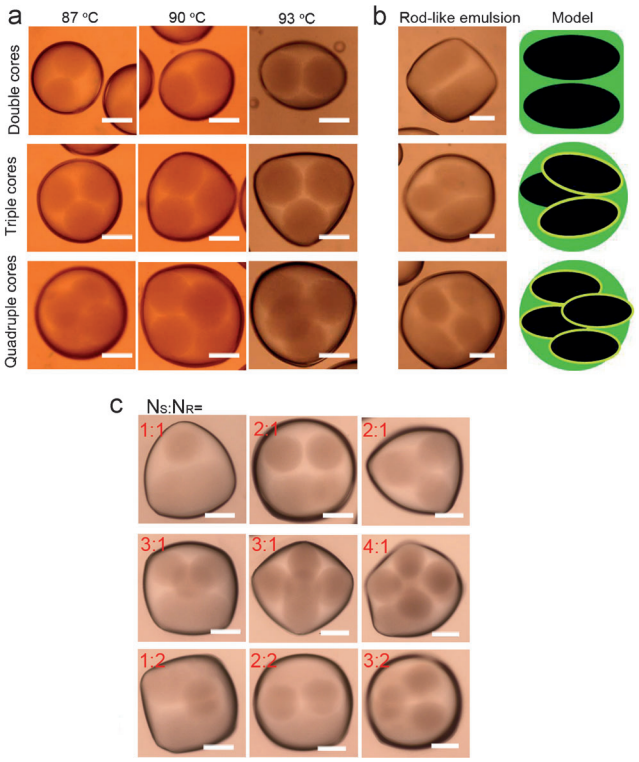

Figure 2. a) Optical microscopy images of the multicore H/W/O emulsion droplets prepared at different temperatures. Optical microscopy images of b) the multiple rodlike core H/W/O emulsion droplets and their schematic illustrations, and c) mixed-shaped core H/W/O emulsion droplets prepared at 93 °C. The MBAM and PEG concentrations are 4 wt% and 10 wt%, respectively. Scale bars: 200 μm.

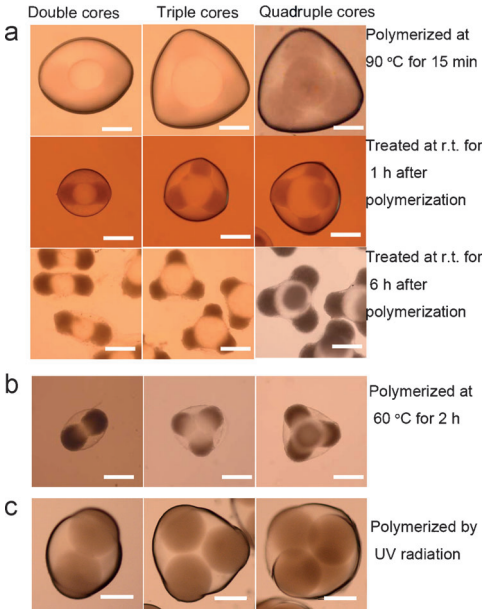

Figure 3. a) Optical microscopy images of the multicore H/W/O hydrogels and hierarchical hydrogel microarchitectures prepared by polymerizing PEGDA at 90 °C for 15 min (top row), after treating in air for 1 h (middle row), and for 6 h (bottom row). Optical microscopy images after b) polymerization at 60 °C for 2 h, and c) polymerization by UV radiation. During the preparation, the multicore H/W/O droplets are prepared at MBAM and PEG concentrations of 4 wt% and 10 wt%, respectively, and a polymerization temperature of 93 °C. Scale bars: 200 μm.

The results above stimulated us to prepare mixed-shape core H/W/O emulsion droplets by fusing spherical core droplets with rod-core droplets. Indeed, the resultant emulsions exhibit distinct configurations depending on the number of spherical core (N_S) and rodlike core (N_R) droplets. The ($N_S = 1$, $N_R = 1$) emulsion droplets show triangle-shaped morphology, while the ($N_S = 2$, $N_R = 1$) droplets exhibit both spherical and triangle-shaped morphologies (Figure 2c), resulting from different arrangements of the cores inside. The ($N_S = 3$, $N_R = 1$) droplets exhibits trapezoid morphology, but with different arrangements of the cores inside (Figure 2c). Irregular-shaped droplets are observed for the ($N_S = 4$, $N_R = 1$) system (Figure 2c). On the other hand, the droplets with two rods as the core do not exhibit big changes in their morphologies, because the two rods are arranged in parallel in the droplet; a square-like shape is observed for the ($N_S = 1$, $N_R = 2$) droplets and a spherical shape for the ($N_S = 2$, $N_R = 2$) and ($N_S = 3$, $N_R = 2$) droplets (Figure 2c).

To convert the above single- and multicore H/W/O emulsions to more easily applicable hydrogels, we fused the H/W/O droplets with one PEGDA droplet, followed by thermally initiated polymerization (Experimental Section 3.3, SI). The H/W/O emulsions were prepared at the polymerization temperature of 93 °C (entry S2, Table S1, SI). We first merged two to four spherical core droplets with a PEGDA droplet and performed the polymerization at 90 °C for 15 min.

The optical microscopy images of the formed hydrogels (top row, Figure 3a) show morphologies similar to those of the corresponding multicore H/W/O emulsion droplets, but with larger particle sizes. The images also show the formation of a round transparent spot at the center of the multicore hydrogels, which pushes the PAM cores to the edge, thus forming inner structures different from those of their corresponding multicore H/W/O emulsion droplets. This probably results from the diffusion of PEGDA into the center of the droplet or thermally induced phase separation of the PEGDA–PEG aqueous system (Figure S5). The PAM cores are not as opaque as those in the emulsions. We let these hydrogels stand at room temperature for 1 h and found no apparent change in the morphology (middle row, Figure 3a). However, the inner structures of the hydrogels are quite different from those of the parent samples before the room temperature treatment; a dumbbell-shape is observed for the double-core hydrogels, a clover-like shape for the triple-core ones, and a tetrahedron-shape for the quadruple-core ones. The PAM cores are more opaque. Apparently, the hydrogels consist of hierarchical-shaped inner structures encapsulated by a transparent shell. The shell is believed to contain much water as it is easy to deform during handling with a stick. After letting these hydrogels stand at room temperature for 6 h, we found that formation of hierarchical hydrogels exhibiting nonspherical microarchitectures had occured (bottom row, Figure 3a). Their morphologies are significantly different from those of the hydrogels treated at room temperature for 1 h, but similar to those of the inner

structures of the above samples. The microarchitectures are assembled around the spherical spot at the core and the previous PAM cores as the vertexes. The PAM cores are opaque. The spherical spot is believed to be poly(PEGDA). To verify this, we added rhodamine B in the PEGDA aqueous droplet to prepare the corresponding microstructured hydrogels and analyzed them by confocal laser scanning microscopy (CLSM). The CLSM images (Figure S6, SI) show red color in the areas without the PAM cores in the hydrogels, suggesting these areas are composed of poly(PEGDA). This can be explained by the affinity of rhodamine B to PEGDA. In addition, the edges of the microarchitectures are also red, indicating that the microarchitectures are formed by encapsulation of polymerized PEGDA. These results indicate that treatment of the hydrogels at room temperature for a long time can tune the morphology of the products, probably resulting from loss of water. We later performed the polymerization of these fused droplets at 60 °C for 2 h and found that the morphology and inner structure of the obtained hydrogels was similar to that of the hydrogels prepared by polymerization at 90 °C for 1 h and treatment at room temperature for 1 h. They also consist of dumbbell-shaped, clover-shaped, and tetrahedron-shaped inner structures encapsulated by a transparent shell for the double-, triple-, and quadruple-core hydrogels (Figure 3b). The shells are not easy to deform and the hydrogels do not deform when they are left at room temperature for a long time, suggesting that the shells are composed of polymerized PEGDA without much water. The emulsions are also polymerized during flow by UV irradiation. (In this case, the APS in the PEGDA aqueous solution was replaced by 2-hydroxy-4′-(2-hydroxyethoxy)-2-methylpropiophenone (IRGACURE2959) with a content of 5 wt % of the PEGDA). The obtained hydrogels show morphologies similar to the corresponding emulsions (Figure 3c). These are different from those of the hydrogels obtained by thermal polymerization, possibly because the polymerization rate by UV irradiation is faster than the PEGDA diffusion rate, or because no phase separation occurred in the PEGDA-PEG system under the preparation conditions. Thus we can control the morphology and structure of the hydrogel by simply choosing the polymerization type and temperature. It should be noted that after soaking in water these hydrogels expand to about twice their original size, with the PAM part swelling significantly more than the poly(PEGDA) part (Figure S7, SI).

We further merged two to four rodlike core droplets with a PEGDA droplet and conducted the polymerization of multiple rodlike core H/W/O droplets at 90 °C for 15 min. The obtained hydrogel shows a general square-like morphology, with two rods being pushed to two edges of the square by a centered ball, forming hamburger-like inner structure (Figure 4a). The obtained hydrogel with three rods exhibits general triangle-morphology, with three parallel aligned rods being pushed to the three edges of the triangle by a centered ball, forming a triangular prism (Figure 4a). The obtained hydrogel with four rods shows a general quadrangular morphology, with the four rods being pushed to the edges (Figure 4a). After the hydrogels were kept at room temperature for more than 6 h, their morphology changes

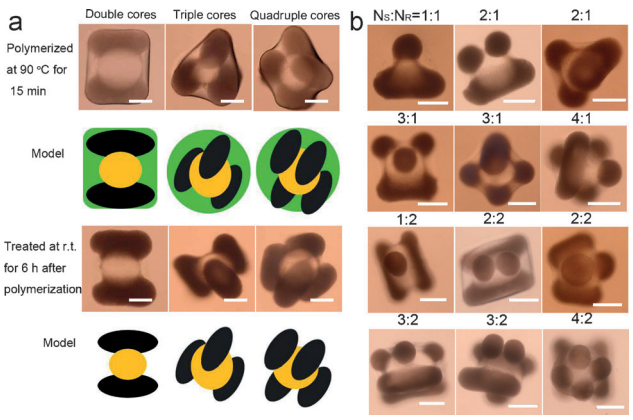

Figure 4. a) Optical microscopy images of the multiple rodlike core H/W/O hydrogels prepared by polymerizing PEGDA at 90 °C for 15 min (top row) and after treating in air for 6 h (bottom row). b) Optical microscopy images of the mixed-shaped hydrogel prepared by polymerizing PEGDA at 90 °C for 15 min, and after treating in air for 6 h. The multicore H/W/O droplets are prepared at MBAM and PEG concentrations of 4 wt % and 10 wt %, respectively, and polymerization temperature of 93 °C. Scale bars: 200 μm.

significantly, without a change in their inner structures (Figure 4a).

We also fused the mixed-shape core H/W/O droplet with a PEGDA droplet, followed by polymerization at 90 °C for 15 min and treatment at room temperature for 6 h. Similar to the above multicore hydrogels, the resultant hydrogels also form a round transparent spot at the center, but quite different morphologies are obtained (Figure 4b). For example, the ($N_S = 1$, $N_R = 1$) hydrogel, whose parent emulsion consists of one spherical core and one rodlike core, shows a T-shaped microstructure. Both the ($N_S = 2$, $N_R = 1$) and ($N_S = 3$, $N_R = 1$) hydrogels also show two different types of morphologies.

To investigate the anisotropy of the hierarchical hydrogels, we examined the adsorption of rhodamine B and CdTe quantum dots in the samples prepared at 90 °C for 15 min (Experimental Section 3.5, SI). The CLSM images of these hydrogels are red at the center after incubation in the rhodamine B solution (top row, Figure 5), green at the vertexes after incubation in the CdTe quantum dots solution (middle row, Figure 5), and both, red at the center and green at the vertexes, after incubation in a mixture of rhodamine B and CdTe quantum dots (bottom row, Figure 5). This is related to the affinity of rhodamine B to PEGDA and the adsorption capacity of PAM for nanoparticles. These results indicate that the hydrogels can be used for efficient selective storage of different functional agents.[36]

We finally investigated the protein-release ability of the hydrogel by using bovine serum albumin (BSA) as a model. Since the thermal polymerization process tends to denature proteins, we tested the hydrogels prepared by photopolymerization with single- and quadruple-core structures (Experimental Section 3.6, SI). The BSA release profiles (Figure 6) show that the protein is quickly released from single-core PAM/PEGDA hydrogels in the first 2 h. Then the release rate slows down with the maximum percentage of BSA release of

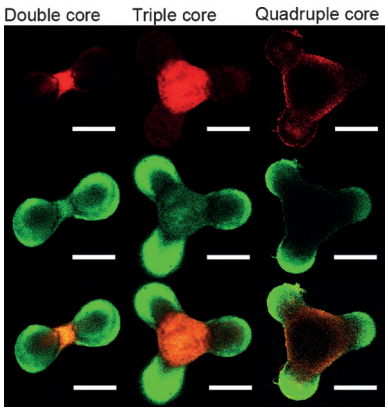

Figure 5. The fluorescent images of the multicore hydrogels after incubation with rhodamine B (top row), with CdTe quantum dots (middle row), and with a mixture of rhodamine B and CdTe quantum dots (bottom row) for 90 s. Scale bars: 250 μm.

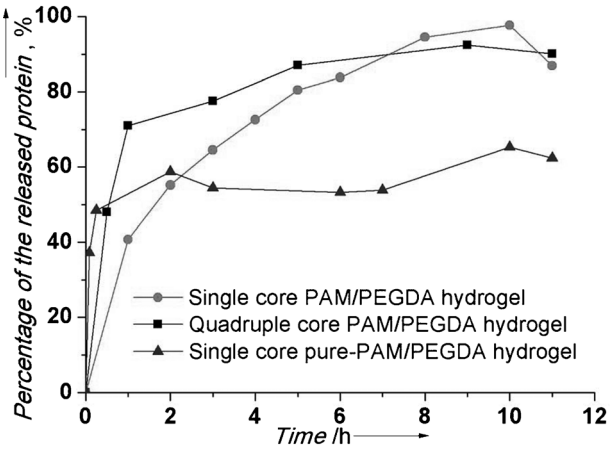

Figure 6. Release of BAS from single- and quadruple-core PAM/PEGDA hydrogels and a single-core pure-PAM/PEGDA hydrogel into acetate buffer at room temperature.

97% at about 8 h. The release rate from the quadruple-core PAM/PEGDA hydrogel is faster than that from single-core hydrogels in the first 1 h, possibly resulting from the thin PEGDA shell around the quadruple-core PAM/PEGDA hydrogel. After 1 h, the release rate slows down, with the maximum percentage of BSA release of 90% at about 5 h. For comparison, we also prepared single-core pure PAM/PEGDA hydrogels without using the phase-separation process. In these hydrogels, the release rate is the fastest in the first 0.5 h and the release of BSA ceases at about 2 h with only 62% protein released. This value is significantly lower than those in the single- and quadruple-core PAM/PEGDA hydrogels. This can be ascribed to the increased BSA accessibility and decreased effective diffusion coefficient in the hydrogels because of the addition of PEG.[37] The results above indicate that the diffusion rate of BSA in the hydrogel can be adjusted by using differently structured hydrogels.

In conclusion, we were able to show that due to phase separation the AM/PEG aqueous droplets form a core/shell structure after polymerization. We thus prepared H/W/O emulsion droplets containing single to multiple PAM cores surrounded by PEG in liquid paraffin and hierarchical PAM/PEG hydrogel microarchitectures with different inner structures and transformable and various morphologies by a simple microfluidic technique. No surfactant is needed in the preparation process. Consequently, coalescence of single-core droplets in an expanding straight channel can be easily accomplished, leading to formation of multicore H/W/O emulsion droplets. The size and morphology of the PAM core can be easily adjusted by changing the polymerization temperatures, leading to an easy adjustment of the morphology of multicore H/W/O emulsion droplets. The emulsions can be converted to corresponding PAM/PEG hydrogels by introducing PEGDA in the system. The hydrogels exhibit different inner structures and various morphologies. The anisotropy of the hydrogel microarchitectures is verified by the adsorption of rhodamine B and CdTe quantum dots. Furthermore, these hydrogels exhibit different release rates of BSA, depending on their structures. Thus, the diffusion rate can be adjusted depending on the desired application. The preparation technique is simple and versatile, and can be easily adjusted by replacing AM with other kinds of acrylamide derivatives or by introducing functional materials separately in different cores. Therefore, the resulting emulsions and hydrogels have potential application for drug release,[38] sensors,[39] and displays,[40] and in biomedical processes.[41]

Received: March 12, 2014
Published online: June 4, 2014

Keywords: emulsions · hydrogels · microfluidics · phase separation · polymers

[1] G. M. Whitesides, *Nature* **2006**, *442*, 368–373.
[2] P. N. Nge, C. I. Rogers, A. T. Woolley, *Chem. Rev.* **2013**, *113*, 2550–2583.
[3] J. T. Wang, J. Wang, J. J. Han, *Small* **2011**, *7*, 1728–1754.
[4] J. H. Xu, S. W. Li, J. Tan, Y. J. Wang, G. S. Luo, *Langmuir* **2006**, *22*, 7943–7946.
[5] A. S. Utada, E. Lorenceau, D. R. Link, P. D. Kaplan, H. A. Stone, D. A. Weitz, *Science* **2005**, *308*, 537–541.
[6] L. Y. Chu, A. S. Utada, R. K. Shah, J. W. Kim, D. A. Weitz, *Angew. Chem. Int. Ed.* **2007**, *46*, 8970–8974; *Angew. Chem.* **2007**, *119*, 9128–9132.
[7] S. H. Kim, D. A. Weitz, *Angew. Chem. Int. Ed.* **2011**, *50*, 8731–8734; *Angew. Chem.* **2011**, *123*, 8890–8893.
[8] a) T. Nisisako, S. Okushima, T. Torii, *Soft Matter* **2005**, *1*, 23–27; b) M. Seo, C. Paquet, Z. H. Nie, S. Q. Xu, E. Kumacheva, *Soft Matter* **2007**, *3*, 986–992.
[9] a) Y. C. Pan, M. H. Ju, C. Q. Wang, L. X. Zhang, N. P. Xu, *Chem. Commun.* **2010**, *46*, 3732–3734; b) S. Y. Teh, R. Khnouf, H. Fan, A. P. Lee, *Biomicrofluidics* **2011**, *5*, 044113; c) S. Ota, S. Yoshizawa, S. Takeuchi, *Angew. Chem. Int. Ed.* **2009**, *48*, 6533–6537; *Angew. Chem.* **2009**, *121*, 6655–6659; d) S. Liu, R. Deng, W. Li, J. Zhu, *Adv. Funct. Mater.* **2012**, *22*, 1692–1697.
[10] a) Y. Liu, M. H. Ju, C. Q. Wang, L. X. Zhang, X. Q. Liu, *J. Mater. Chem.* **2011**, *21*, 15049–15056; b) Y. Wang, E. Tumarkin, D. Velasco, M. Abolhasani, W. Lau, E. Kumacheva, *Lab Chip* **2013**, *13*, 2547–2553; c) Y. Chen, G. Nurumbetov, R. Chen, N. Ballard, S. A. F. Bon, *Langmuir* **2013**, *29*, 12657–12662; d) J. Wang, Y.

Hu, R. Deng, W. Xu, S. Liu, R. Liang, Z. Nie, J. Zhu, *Lab Chip* **2012**, *12*, 2795 – 2798.
[11] S. N. Yin, C. F. Wang, Z. Y. Yu, J. Wang, S. S. Liu, S. Chen, *Adv. Mater.* **2011**, *23*, 2915 – 2919.
[12] Y. J. Zhao, H. C. Gu, Z. Y. Xie, H. C. Shum, B. P. Wang, Z. Z. Gu, *J. Am. Chem. Soc.* **2013**, *135*, 54 – 57.
[13] S. Seiffert, M. B. Romanowsky, D. A. Weitz, *Langmuir* **2010**, *26*, 14842 – 14847.
[14] T. H. Eun, S. H. Kim, W. J. Jeong, S. J. Jeon, S. H. Kim, S. M. Yang, *Chem. Mater.* **2009**, *21*, 201 – 203.
[15] a) W. Wang, M. J. Zhang, R. Xie, X. J. Ju, C. Yang, C. L. Mou, D. A. Weitz, L. Y. Chu, *Angew. Chem. Int. Ed.* **2013**, *52*, 8084 – 8087; *Angew. Chem.* **2013**, *125*, 8242 – 8245; b) B. Kim, H. S. Lee, J. Kim, S. H. Kim, *Chem. Commun.* **2013**, *49*, 1865 – 1867.
[16] D. Lee, D. A. Weitz, *Small* **2009**, *5*, 1932 – 1935.
[17] J. C. Baret, *Lab Chip* **2012**, *12*, 422 – 433.
[18] N. N. Deng, Z. J. Meng, R. Xie, X. J. Ju, C. L. Mou, W. Wang, L. Y. Chu, *Lab Chip* **2011**, *11*, 3963 – 3969.
[19] S. C. Glotzer, M. J. Solomon, *Nat. Mater.* **2007**, *6*, 557 – 562.
[20] Y. Qiu, K. Park, *Adv. Drug Delivery Rev.* **2012**, *64*, 49 – 60.
[21] C. A. Serra, I. U. Khan, Z. Q. Chang, M. Bouquey, R. Muller, I. Kraus, M. Schmutz, T. Vandamme, N. Anton, C. Ohm, R. Zentel, A. Knauer, M. Köhler, *J. Flow Chem.* **2013**, *3*, 66 – 75.
[22] A. Kumachev, J. Greener, E. Tumarkin, E. Eiser, P. W. Zandstra, E. Kumacheva, *Biomaterials* **2011**, *32*, 1477 – 1483.
[23] W. H. Tan, S. Takeuchi, *Adv. Mater.* **2007**, *19*, 2696 – 2701.
[24] a) B. G. Chung, K. H. Lee, A. Khademhosseini, S. H. Lee, *Lab Chip* **2012**, *12*, 45 – 49; b) D. Dendukuri, T. A. Hatton, P. S. Doyle, *Langmuir* **2007**, *23*, 4669; c) V. Palermo, P. Samori, *Angew. Chem. Int. Ed.* **2007**, *46*, 4428 – 4432; *Angew. Chem.* **2007**, *119*, 4510 – 4514.
[25] a) H. C. Shum, A. R. Abate, D. Lee, A. R. Studart, B. Wang, C. H. Chen, J. Thiele, R. K. Shah, A. Krummel, D. A. Weitz, *Macromol. Rapid Commun.* **2010**, *31*, 108 – 118; b) Z. H. Nie, W. Li, M. Seo, S. Q. Xu, E. Kumacheva, *J. Am. Chem. Soc.* **2006**, *128*, 9408 – 9412; c) Z. H. Nie, S. Q. Xu, M. Seo, P. C. Lewis, E. Kumacheva, *J. Am. Chem. Soc.* **2005**, *127*, 8058 – 8063; d) T. Nisisako, T. Torii, T. Takahashi, Y. Takizawa, *Adv. Mater.* **2006**, *18*, 1152 – 1156.
[26] A. X. Lu, K. Jiang, D. L. DeVoe, S. R. Raghavan, *Langmuir* **2013**, *29*, 13624 – 13629.
[27] J. Kim, S. A. Vanapalli, *Langmuir* **2013**, *29*, 12307 – 12316.
[28] S. S. Lee, A. Abbaspourrad, S. H. Kim, *ACS Appl. Mater. Interfaces* **2014**, *6*, 1294 – 1300.
[29] A. R. Studart, H. C. Shum, D. A. Weitz, *J. Phys. Chem. B* **2009**, *113*, 3914 – 3919.
[30] B. G. Wang, H. C. Shum, D. A. Weitz, *ChemPhysChem* **2009**, *10*, 641 – 645.
[31] S. H. Kim, H. Hwang, C. H. Lim, J. W. Shim, S. M. Yang, *Adv. Funct. Mater.* **2011**, *21*, 1608 – 1615.
[32] C. H. Chen, R. K. Shah, A. R. Abate, D. A. Weitz, *Langmuir* **2009**, *25*, 4320 – 4323.
[33] N. Prasad, J. Perumal, C. H. Choi, C. S. Lee, D. P. Kim, *Adv. Funct. Mater.* **2009**, *19*, 1656 – 1662.
[34] A. Y. Kwok, E. L. Prime, G. G. Qiao, D. H. Solomon, *Polymer* **2003**, *44*, 7335 – 7344.
[35] a) Y. Zhang, H. Liu in *Microdroplet Technology*, Springer, Heidelberg, **2012**, pp. 14 – 15; b) Y. C. Tan, J. S. Fisher, A. I. Lee, V. Cristini, A. P. Lee, *Lab Chip* **2004**, *4*, 292 – 298.
[36] C. H. Choi, D. A. Weitz, C. S. Lee, *Adv. Mater.* **2013**, *25*, 2536 – 2541.
[37] A. G. Lee, C. P. Arena, D. J. Beebe, S. P. Palecek, *Biomacromolecules* **2010**, *11*, 3316 – 3324.
[38] H. G. Schild, *Prog. Polym. Sci.* **1992**, *17*, 163 – 249.
[39] D. Buengera, F. Topuza, J. Groll, *Prog. Polym. Sci.* **2012**, *37*, 1678 – 1719.
[40] Z. Yu, C. F. Wang, L. Ling, L. Chen, S. Chen, *Angew. Chem. Int. Ed.* **2012**, *51*, 2375 – 2378; *Angew. Chem.* **2012**, *124*, 2425 – 2428.
[41] A. S. Hoffman, *Adv. Drug Delivery Rev.* **2002**, *54*, 3 – 12.

